BIPOLAR ELECTROSTATIC DRIVING FOR HIGH-RESOLUTION ISOLATED BATTERY VOLTAGE SENSOR

Naoki Nobunaga[1], Shinya Kumagai[1], Hiroki Ishihara[2], Makoto Ishii[2], and Minoru Sasaki[1]
[1] Toyota Technical Institute, Nagoya, Aichi, JAPAN
[2] Yazaki Corporation, Susono, Shizuoka, JAPAN

ABSTRACT

Si resonator is applied for measuring the voltage in a highly isolated manner. The resonant frequency shift being affected by the electrical field from the high voltage (supposing the battery) is the working principle. Here, the resonator is electrically floated for the isolation and the outside driving voltage is set to be bipolar for avoiding the fluctuation which will be caused by charging of the resonator. This new method stabilizes the resonant frequency realizing 0.25V accuracy at 80V. Feasibility for measuring the high voltage up to 420V is demonstrated.

INTRODUCTION

For introducing the renewable energy in the daily life, the energy management becomes further important[1]. The solar or wind powers are typical ones, but their output changes so much depending on the weather condition. This is troublesome for obtaining the balance between the demand and the supply. For realizing the delicate control of the power flow, the sensors to measure current and voltage become indispensable. In the smart grid, the batteries absorbing or supplying the energy will be familiar in the smart house, the electrical vehicle, and so on. The electric power is measured by the current and the voltage sensors, which are required to be short-proof, power-saving, and small[2]. As for the isolated current sensing, measuring the magnetic field can be the solution based on the Biot-Savart law. Hall magnetic sensors can measure the current in a non-contact manner [3]. For reducing the Joule's loss, the voltage in the power system will be higher. The data center will use 380V. Figure 1(a) shows the typical method dividing the high voltage to the smaller one using the resistances. Measuring the small voltage divided by resistances from the power line needs the temperature compensation. This doesn't avoid the risk of shortage because the current path exists. So, the isolation circuit becomes necessary. As shown in Fig. 1(b), the sensing without the direct current path is required for the safety. In case of the battery, it is also for avoiding the power consumption. There is no strong sensor candidate. The sensors based on Pockels crystal is complicated due to the necessity of the optical setup [4, 5, 6]. DC electrostatic filed sensors based on the field mill principle is tried to be miniaturized using the shutter microactuator although the effect removing spurious offsets, drifts, and space charge is not perfect [7, 8, 9].

We have proposed a new voltage sensor based on the change of the resonant frequency caused by the gradient of the electrostatic force[10, 11]. However, the measurement accuracy is not high. In this study, the combination of the electrically floated resonator and the bipolar electrostatic driving is newly applied for the stability and the higher resolution.

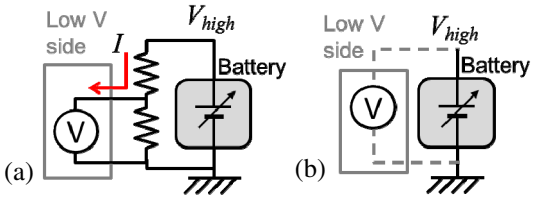

Figure 1: (a) Conventional method for measuring the high voltage dividing the total voltage to the smaller one for sensing. (b) The model of the isolated voltage sensing.

SENSING PRINCIPLE

The phenomenon decreasing the resonant frequency by applying the electrical field is known and used in the gyro sensors for tuning the resonant frequency [12]. The electrostatic force generated between the parallel plate electrodes increases when the electrode gap decreases. When the vibration amplitude is small, the slope near the operation point can be approximated to be constant. This slope has the same dimension of that of the spring constant (force per distance), and its value is negative. The magnitude of this negative spring constant becomes larger when the gap decreases as well as when the applied voltage increases. This negative spring constant cancel the mechanical spring constant. So, the resonant frequency decreases. Considering the parallel prate actuator as shown in Fig. 2(a), using the resonant frequency f_0 at 0V and the pull-in voltage $V_{pull\text{-}in}$ as the normalizing factors, the voltage and the resonant frequency can be written by the equations (1) and (2) using the displacement of the moving electrode x[8].

$$\left(\frac{V_{high}}{V_{pull-in}}\right)^2 = \frac{27}{4}\frac{x}{g}\left(1-\frac{x}{g}\right)^2 \quad (1)$$

$$f_r = f_0\sqrt{\frac{1-3x/g}{1-x/g}} \quad (2)$$

Figure 2(b) shows the theoretical curve of the resonant frequency f_r when V_{high} is applied[4]. The decreasing ratio of the frequency is small at the lower voltage and large at the larger voltage especially at around the pull-in voltage. From the decrease of the resonant frequency, the applied voltage can be obtained.

The potential V_f of the resonator is decided by the relative position against the surrounding electrodes which are connected to the fixed potentials. When the resonator displaces by x approaching to the electrode with high potential as shown in Fig. 2(a), the floating potential V_f will be higher value. The model shown in Fig. 2(a) gives the potential as follows.

$$V_f = \frac{g_1 + x}{g}\cdot\left(V_{high} - V_{drive}e^{j\omega t}\right) \quad (3)$$

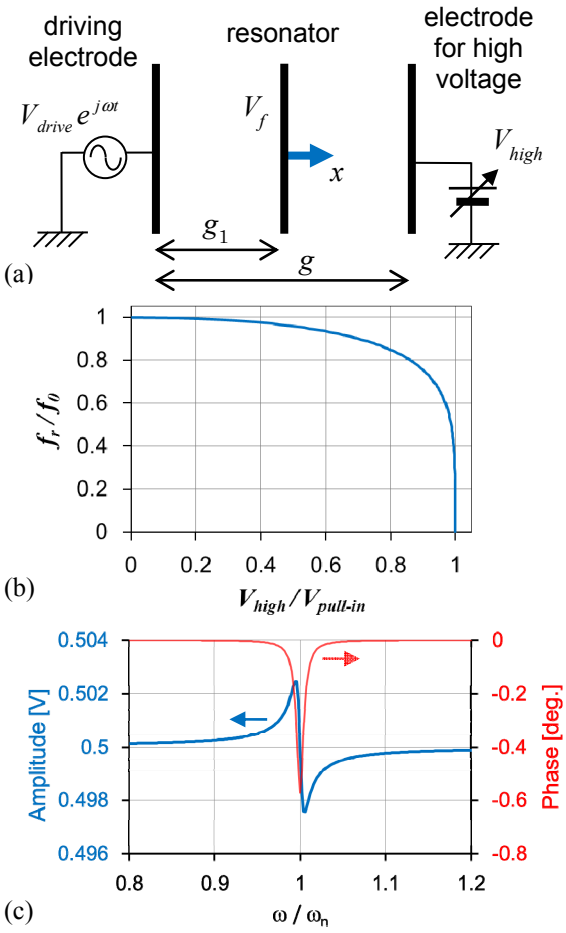

Figure 2: (a) Analytical model for the floating potential generated on the resonator. (b) Theoretical curve of the resonant frequency shift generated by the voltage causing the electrostatic attraction. The frequency and the voltage are normalized by the initial resonant frequency and the pull-in voltage, respectively. (c) Theoretical frequency response of the floating potential generated on the resonator.

The displacement x of the resonator can be expressed as follows.

$$x = \frac{x_{st}}{1-\left(\frac{\omega}{\omega_n}\right)^2 + j2\zeta\frac{\omega}{\omega_n}} \tag{4}$$

Figure 2(c) shows the amplitude and the phase of V_f supposing the parameter listed in Table 1. Around the resonant frequency, the amplitude curve has the pair of up and down peaks. The phase has the valley. This sharpness of the resonator shows Q value.

FABRICATION

Figure 3 shows the fabrication sequence based on the standard SOI(silicon-on-insulator)-MEMS process etching the Si material from both sides and releasing the resonator. (1) The starting is SOI wafer. (2) The relatively fine pattern of the resonator is transferred to the device layer. (3) The deep-RIE (Reactive Ion Etching) is carried out. The finest pattern size of 3μm in the suspension becomes 2.95μm in the actual size. The narrowest gap is 5.15μm. The aspect ratio is designed to be lower than 10 for progressing the Si etching uniformly. (4) The handle layer is patterned. This pattern opens the space at the bottom of the resonator. This will reduce the dumping. The resist film is UV cured making its property to be inert against the thinner and the developer. Then the additional resist film is coated and patterned. This is for making the resist mask thicker. (5) The deep-RIE is carried out to the handle layer. (6) The appeared oxide layer is removed using the buffered HF. (7) The vapor HF etching is carried out for releasing the resonator. (8) Al layer is deposited using the stencil mask on the contact area. The sintering is carried out. This is for obtaining the electrical contact.

Table 1: Parameters used in the analytical model.

Parameter	Symbol	Supposed value
Static displacement	x_{st}	1 nm
Angular resonant frequency	ω_n	2π x 20 kHz
Inverse of Q	2ζ	0.01
Total gap	g	20 μm
Driving electrode -resonator gap	g_1	10 μm
High voltage to be measured	V_{high}	100 V
Amplitude of the driving voltage	V_{drive}	10 V

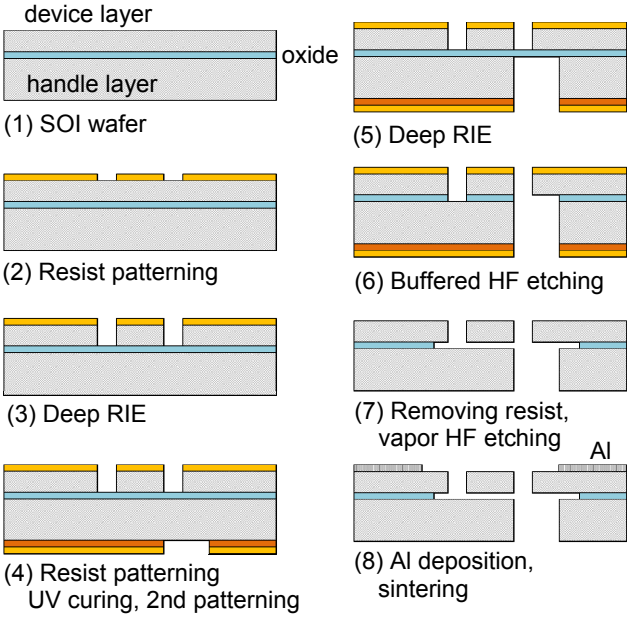

Figure 3: Fabrication sequence.

Figure 4(a) shows the whole view of one fabricated device. The Si structures are vertically etched. Although the Al metal is a little shifted from the designed position, Al metal patterns are on the electrode pads. The driving circuit is included. Figure 4(b) shows the magnified view of the resonator and the surrounding parallel and comb electrodes. The gap between the resonator and the electrode for applying the high voltage is 10 μm. For decreasing the discharging risk, the electrode for applying

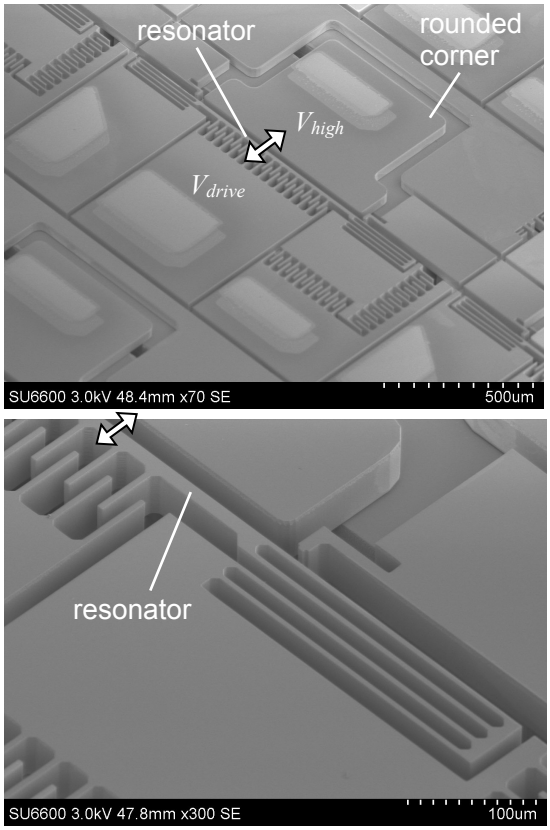

(a)

(b)

Figure 4: One of devices fabricated. Al metal on the top is deposited on the electrode pads for the electrical contact.

the high voltage has the rounded corners. The lateral gap is 60 µm wider to the other gap.

EXPERIMENTAL SETUP

Figure 5 shows the setup for the device. The measurement is electrical. The frequency response analyzer (NF corp., FRA5097) is used. The output signal from FRA is amplified and applied to the driving electrode. The induced voltage is measured across the blocking capacitance which avoids the dc current for keeping the voltage value. Probing station is combined with the vacuum chamber for controlling the environment. The pressure can decrease to 1.2×10^{-3} Pa. The lower pressure can increase Q and the signals of up and down peaks.

RESULTS

Figure 6 shows the typical response of the induced voltage. As expected in the theory in Fig. 2, there is the paired up and down peaks. The phase change is also similar to that shown in Fig. 2, although it is not shown here. With the voltage, the resonant frequency decreases.

Figure 7 shows the case when the driving voltage is positive (the sinusoidal curve with the offset to make the monopole voltage). At each condition of the measurement voltage, there are 10 data for showing the distribution. The resonant frequency fluctuates time to time. This fluctuation becomes the error of the measurement voltage. The fluctuation exists even at 0V of the measurement voltage. The data distribution seems to increase when the

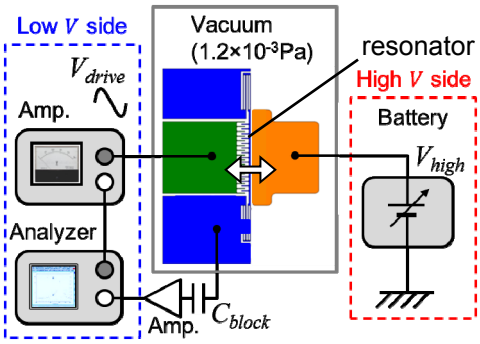

Figure 5: Experimental setup and the driving circuit for the sensor.

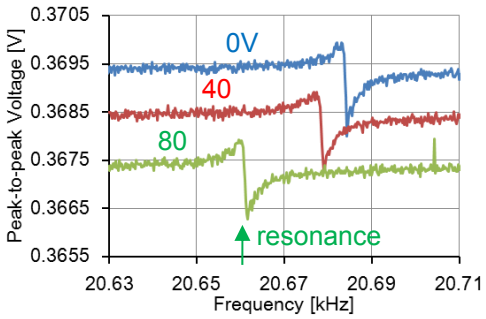

Figure 6: Typical response of the induced ac voltage on the resonator measured in vacuum.

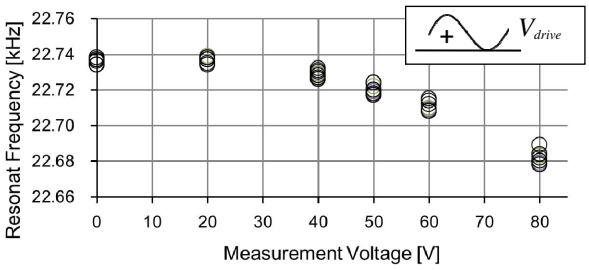

Figure 7: Resonant frequency measured with the unipolar driving voltage measured in vacuum.

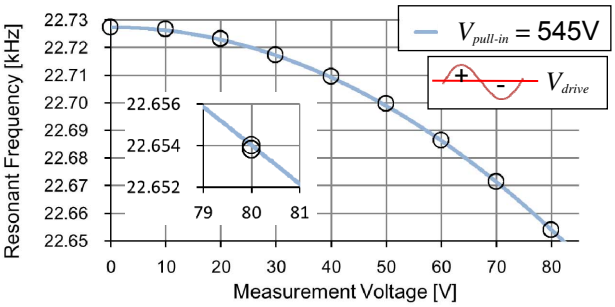

Figure 8: Resonant frequency measured with the bipolar driving voltage measured in vacuum. The effective driving frequency is double of that of the electrical one.

measurement voltage V_{high} increases.

Figure 8 shows the case when the driving voltage is bipolar having the average of 0V. The solid theoretical curve supposes the pull-in voltage of 545V based on the equations (1) and (2). They agree well each other. The inset is the magnified curve at around 80V. There are 10 data, and many of them are same value. At 80V, the fluctuation corresponds to only 0.25V. There is no hysteresis observed

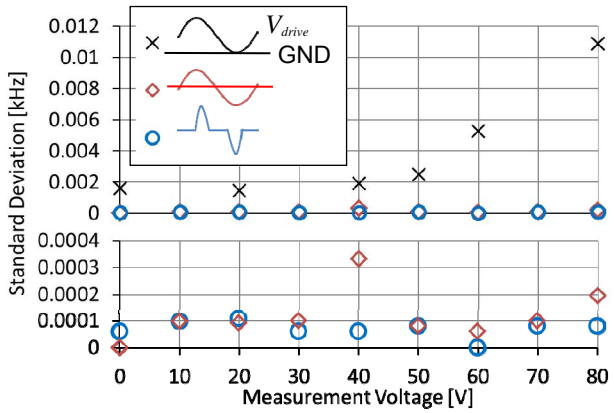

Figure 9: Standard deviations of the resonant frequency measured using 3 different driving waveforms (monopolar voltage, bipolar voltage, and bipolar voltage with 0V plateau). The lower is the magnified data.

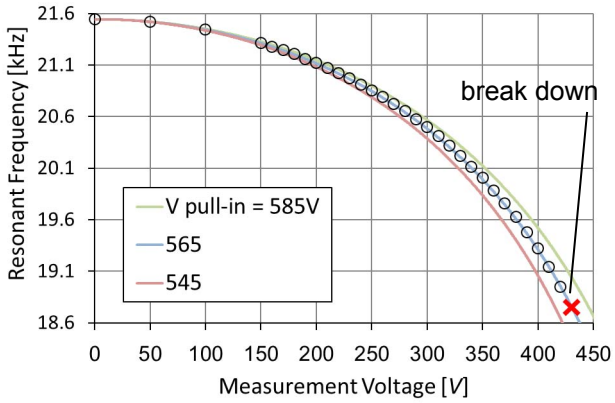

Figure 10: Voltage measurement up to 420V. The break down occurs at 430V before the pull-in.

when the measurement voltage increases and decreases. Figure 9 shows the standard deviation with different driving waveforms. The main reason of the fluctuation is considered to be the charging of the resonator. When the driving waveform has 0V plateau in a cycle, the standard deviation further reduces to less than 0.1Hz.

Figure 10 shows the case when the voltage V_{high} up to 420V (>380V) is measured using the bipolar driving voltage. The solid theoretical curves supposes the pull-in voltages at 585, 565, and 545V. The experimental data clearly follow the curve for the pull-in voltage of 565V. At 430V, the discharging break down occurs.

CONCLUSION

A high-resolution isolated battery voltage sensor is realized using the Si resonator. The measuring method doesn't need the current from the battery. Since the electrical field from the electrode connected to the battery output influences the resonant frequency of the resonator, the voltage can be measured. For the isolation, the resonator is set to be electrically isolated. On the other hand, the resonator can be charged disturbing the measurement accuracy. By applying the outside driving voltage to be bipolar, the data fluctuation decreases. This new method stabilizes the resonant frequency realizing 0.25V accuracy at 80V. Feasibility for measuring the high voltage up to 420V is demonstrated.

ACKNOWLEDGEMENTS

Part of this research was supported by MEXT program for Forming Strategic Research Infrastructure (S1311034).

REFERENCES

[1] R. Abe, H. Taoka, D. McQuilkin, "Digital grid: Communicative electrical grids of the future", IEEE Trans. Smart Grid, Vol. 2, No. 2 (2011) pp.399-410.

[2] Y. C. Chen, W. H. Hsu, S. H. Cheng, Y. T. Cheng, "A Power Sensor Tag With Interference Reduction for Electricity Monitoring of Two-Wire Household Appliances", IEEE Trans. on Industrial Electronics, Vol. 61, No. 4 (2014) 2062-2070.

[3] I. Shibasaki, "Thin film Hall element widely used in daily life", Oyo Butsuri, Vol. 90, No. 1 (2011) pp.36-41 (in Japanese).

[4] M. Higaki, S. Yamaguchi, "Optical DC Voltage Measurement Based on AC Voltage Modulation of Elliptically Polarized Light Using BGO Crystals", Trans. Inst. Elect. Eng. Japan. B, Vol. 117, No. 5 (1997) pp.634-640 (in Japanese).

[5] J. C. Santos, M. C. Taplamacioglu, K. Hidaka, "Optical high voltage measurement using Pockels microsingle crystal", Rev. Sci. Instrum. Vol. 70, No.8 (1999) pp.3271-3276.

[6] F. Pan, X. Xiao, Y. Xu, S. Ren, "An Optical AC Voltage Sensor Based on the Transverse Pockels Effect", Sensors 2011, Vol. 11, No. 7, pp.6593-6602.

[7] S. J. Sawa, "A MEMS-based, high-resolution Electric-Field meter", Thesis (M. Eng.), Massachusetts Institute of Technology (2005).

[8] R. Miles, T. Bond, G. Meyer, "Report on Non-Contact DC Electric Field Sensors", LLNL-TR-414129 (2009).

[9] C. Peng C. Peng, P. Yang P. Yang, H. Zhang H, Zhang, X. Guo X. Guo, S. Xia S. Xia, "Design of a SOI MEMS resonant electric field sensor for power engineering applications", Proc. IEEE Sensors. Conf. (2010) pp.1183-1186.

[10] S. Hasegawa, S. Kumagai, M. Sasaki, "Non-Contact Voltage Measurement Using a Micro –Resonator", IEEJ Trans. on Sens. Micromachines E, Vol. 133, No.8 (2013) pp.354-358.

[11] N. Nobunaga, S. Hasegawa, S. Kumagai, K. Masuno, M. Ishii, S. Uematsu, M. Sasaki, "Isolated Voltage Sensing Using Micro-Resonator", The 17th International Conference on Solid-State Sensors, Actuators and Microsystems T3P.113 (2013) pp.1360-1363.

[12] Y. He, J. Marchetti, C. Gallegos, F. Maseeh, "Accurate Fully-Coupled Natural Frequency Shift of MEMS Actuators Due to Voltage Bias and Other External Forces", Proc. 12th IEEE Int. Conf. on Micro Electro Mechanical Systems (1999) pp.321-325.

CONTACT

*M. Sasaki, tel: +81-52-809-1840; mnr-sasaki@ toyota -ti.ac.jp